J|A|C|S ARTICLES

Published on Web 08/19/2009

The Role of Gold Adatoms and Stereochemistry in Self-Assembly of Methylthiolate on Au(111)

Oleksandr Voznyy,*,† Jan J. Dubowski,† J. T. Yates, Jr.,‡,§ and Peter Maksymovych*,§,||

Department of Electrical and Computer Engineering, Centre of Excellence for Information Engineering (CEGI), Université de Sherbrooke, Sherbrooke, Québec J1K 2R1, Canada, Department of Chemistry, University of Virginia, Charlottesville, Virginia 22904, Department of Chemistry, University of Pittsburgh, Pittsburgh, Pennsylvania 15217, and Center for Nanophase Materials Sciences, Oak Ridge National Laboratory, Oak Ridge, Tennessee 37831

Received April 2, 2009; E-mail: o.voznyy@usherbrooke.ca; 5 nm@ornl.gov

Abstract: On the basis of high resolution STM images and DFT modeling, we have resolved low- and high-coverage structures of methylthiolate (CH_3S) self-assembled on the Au(111) surface. The key new finding is that the building block of all these structures has the same stoichiometry of two thiolate species joined by a gold adatom. The self-arrangement of the methylthiolate−adatom complexes on the surface depends critically on their stereochemical properties. Variations of the latter can produce local ordering of adatom complexes with either (3×4) or $(3 \times 4\sqrt{3})$ periodicity. A possible structural connection between the $(3 \times 4\sqrt{3})$ structure and commonly observed $(\sqrt{3} \times \sqrt{3})R30°$ phase in methylthiolate self-assembled monolayers is developed by taking into account the reduction in the long-range order and stereochemical isomerization at high coverage. We also suggest how the observed self-arrangements of methylthiolate may be related to the $c(4 \times 2)$ phase of its longer homologues.

1. Introduction

Molecular self-assembly is a quickly developing field of nanoscience that aims to tailor self-recognizing and self-organizing properties of molecules for the bottom-up construction of complex molecular systems and implementation of the designer molecular functionality. The greatest attention has been devoted to the self-assembly of alkylthiolates (general formula $C_nH_{2n+1}S$) on gold surfaces, which yields three-dimensional crystalline monolayers with molecular tails decoupled from the metal substrate.[1] These unique properties have enabled a great variety of alkanethiol-based applications, including molecular electronics, immobilization of biomolecules, surface magnetism, passivation of nanoparticles and so forth (see ref 2 and references therein). However, despite the apparent simplicity of the self-assembly process, commonly regarded as an evolution of the packing order upon increasing surface coverage of the adsorbate, almost every aspect of alkanethiol self-assembly on Au(111) remains controversial.[3]

Until only recently, the gold surface has been considered a passive template which provides a series of high-symmetry adsorption sites for the alkylthiolate species.[1,4−8] However, it is now well-established that the bonding of the sulfur headgroup to the Au(111) surface involves Au-adatoms.[9−12] The Au-adatoms are supplied by lifting the herringbone reconstruction of the Au(111) surface,[9] as well as etching of the monatomic steps and terraces[7] upon thiolate self-assembly. In our recent publication based on scanning probe imaging,[9] it was found that the elementary building block of the self-assembled methylthiolate phase at low coverage is a CH_3S−Au(adatom)--SCH_3 species. A similar motif was subsequently found in the self-assembly of benzenethiolate on Au(111)[13] as well as in the bonding of arenethiolates to gold nanoparticles.[14] Au-adatoms provide a significant contribution to the energy of the anchor-bond,[9,15,16] and it is therefore very likely that they will influence the self-assembly process at all coverages and stability

† Université de Sherbrooke.
‡ University of Virginia.
§ University of Pittsburgh.
|| Oak Ridge National Laboratory.

(1) Schreiber, F. *Prog. Surf. Sci.* **2000**, *65*, 151–256.
(2) Love, J. C.; Estroff, L. A.; Kriebel, J. K.; Nuzzo, R. G.; Whitesides, G. M. *Chem. Rev.* **2005**, *105*, 1103–1169.
(3) Woodruff, D. P. *Phys. Chem. Chem. Phys.* **2008**, *10*, 7211–7221.
(4) Poirier, G. E.; Pylant, E. D. *Science* **1996**, *272*, 1145–1148.
(5) Kondoh, H.; Iwasaki, M.; Shimada, T.; Amemiya, K.; Yokoyama, T.; Ohta, T.; Shimomura, M.; Kono, S. *Phys. Rev. Lett.* **2003**, *90*, 066102–066105.
(6) Gronbeck, H.; Curioni, A.; Andreoni, W. *J. Am. Chem. Soc.* **2000**, *122*, 3839–3842.
(7) Zhang, J. D.; Chi, Q. J.; Ulstrup, J. *Langmuir* **2006**, *22*, 6203–6213.
(8) Torrelles, X.; Barrena, E.; Munuera, C.; Rius, J.; Ferrer, S.; Ocal, C. *Langmuir* **2004**, *20*, 9396–9402.
(9) Maksymovych, P.; Sorescu, D. C.; Yates, J. T. *Phys. Rev. Lett.* **2006**, *97*, 146103–146106.
(10) Mazzarello, R.; Cossaro, A.; Verdini, A.; Rousseau, R.; Casalis, L.; Danisman, M. F.; Floreano, L.; Scandolo, S.; Morgante, A.; Scoles, G. *Phys. Rev. Lett.* **2007**, *98*, 016102–016105.
(11) Yu, M.; Bovet, N.; Satterley, C. J.; Bengio, S.; Lovelock, K. R. J.; Milligan, P. K.; Jones, R. G.; Woodruff, D. P.; Dhanak, V. *Phys. Rev. Lett.* **2006**, *97*, 166102–166105.
(12) Kautz, N. A.; Kandel, S. A. *J. Am. Chem. Soc.* **2008**, *130*, 6908–6909.
(13) Maksymovych, P.; Yates, J. T., Jr. *J. Am. Chem. Soc.* **2008**, *130*, 7518–7519.
(14) Jadzinsky, P. D.; Calero, G.; Ackerson, C. J.; Bushnell, D. A.; Kornberg, R. D. *Science* **2007**, *318*, 430–433.
(15) Gronbeck, H.; Hakkinen, H.; Whetten, R. L. *J. Phys. Chem. C* **2008**, *112*, 15940–15942.

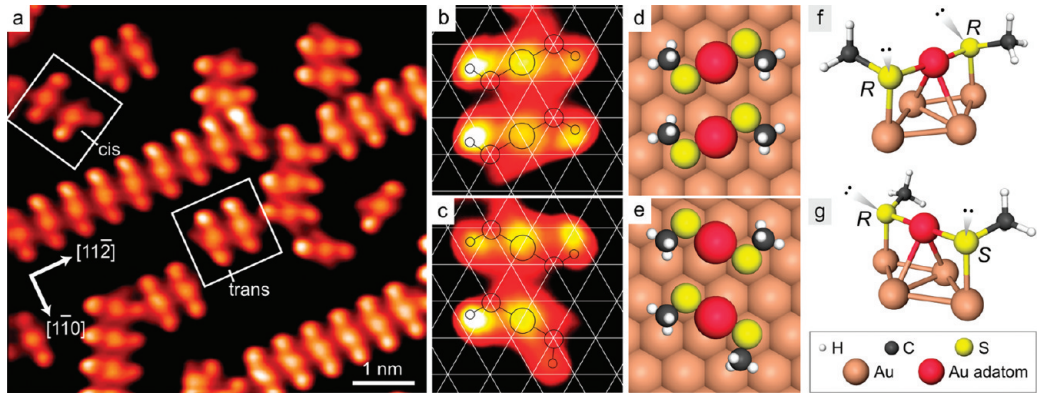

Figure 1. STM images of self-assembled structures of methylthiolate at low coverage on Au(111), produced by heating the gold crystal predosed with CH_3SSCH_3 above 200 K for ~10 min (a). Triangulation of two *trans*-$(CH_3S)_2Au$ complexes (b) and adjacent *cis*- and *trans*-adatom complexes (c), and their schematic models (d) and (e), respectively. The known adsorption sites of the adatom-complexes[9] and the orientation of the 1D-stripes were used to derive the relative location of the surface lattice (hexagonal mesh). DFT-optimized structures of (*R*,*R*)-*trans* (f) and (*R*,*S*)-*cis* (g) configurations. The formal *R*-configuration of sulfur is assigned based on the following order: lone electron pair, CH_3, surface Au atom (other surface atoms are not considered), Au adatom (connected to the other CH_3S fragment).

of thiolate species against desorption. So far, very little direct evidence has been obtained as to what role Au-adatoms play in the intermediate 2D-monolayers, the so-called striped phases,[1,4] and whether the sulfur−gold bonding changes as the coverage of thiolates on gold surfaces approaches saturation. For the saturation coverage, several models have been proposed, involving thiolate species bonded atop Au-adatoms,[11] thiolate−adatom−thiolate complexes akin those observed at low coverage,[15] polymer-like adatom−thiolate complexes[17,18] or a dynamic equilibrium between adatom-bonded and bridge-bonded alkylthiolates adjacent to vacancy.[10,19] In addition, at least three kinds of symmetry were reported in alkanethiolate SAMs, depending on the length of the hydrocarbon chains:[1] ($\sqrt{3} \times \sqrt{3}$)*R*30°, ($3 \times 2\sqrt{3}$) (which is a $c(4 \times 2)$ superstructure of the $\sqrt{3}$ symmetry) and (3×4). The mechanism of self-assembly leading to this variety of structures remains unresolved and demands further exploration.

In this paper, we present a combined study of the intermediate and high coverage structures of short-chain alkylthiolates on Au(111) using scanning tunneling microscopy (STM) and density-functional theory (DFT). We describe underappreciated inherent chirality of the low coverage (striped) phase and observe how it manifests in the structure evolution at higher coverages. We develop a unified picture where the methylthiolate SAMs at all coverages are built of compositionally the same unit ($CH_3S-Au-SCH_3$), while its stereochemical properties play a critical role in determining the order within the self-assembled structure.

2. Methods

The experiments were conducted with a low-temperature STM (Omicron) operating in an ultrahigh vacuum (UHV) chamber (background pressure $<5.0 \times 10^{-11}$ Torr). The Au(111) surface (in our case a facet of a single crystal at the end of a gold wire[20]) was cleaned by Ar^+ sputtering and annealing to 773 K. The clean gold surfaces exhibited a terrace size of 1−2 μm and a ($22 \times \sqrt{3}$) herringbone reconstruction with no surface impurity adsorbates visible in the elbow sites.[21] The CH_3SSCH_3, CH_3SH and C_3H_7SH were purified using several freeze−pump−thaw cycles. Each compound was deposited on the surface through an effusive beam doser while the crystal was in the STM imaging position at <10 K. The surface was subsequently heated to higher temperatures where molecular dissociation and self-assembly occurred, as described further in text. All the STM images presented here were taken at a temperature of 5K.

The DFT calculations were performed using scalar-relativistic pseudopotentials with nonlinear core corrections, within the generalized gradient approximation (GGA) as implemented in the SIESTA code.[22] The surface slab was modeled with 5 Au layers and a vacuum region of 30 Å. A (4×5) Monkhorst-Pack k-grid was used for Brillouin zone sampling. More calculation details can be found in previous works.[23]

3. Results and Discussion

Methylthiolate species was previously found to chemisorb on the Au(111) surface in the form of the CH_3S-Au-(adatom)$-SCH_3$ complex at temperatures above ~200 K (hereafter $(CH_3S)_2Au$ or *adatom complex*) with the S-atom forming three covalent bonds:[9] S−C to the methyl group, S−Au to the adatom and S−Au to the gold atom in the surface, as shown in Figure 1. The S-atom is positioned beside the Au-adatom and atop the surface Au-atom (Figure 1d,e), providing for an agreement with the original findings of the atop bonding by the spectroscopic measurements using photoelectron diffraction (PED)[5] and normal incidence X-ray standing wave (NIXSW).[3,11] For the purpose of the following discussion, it is convenient to consider sp^3-like hybridization of the S-atoms in the adatom complex,[24] where three orbitals participate in the bonding and the fourth one contains a lone electron pair. The S-atom is thus formally chiral and can be designated as being *R*- or *S*-type using the standard stereochemical nomenclature

(16) Wang, Y.; Hush, N. S.; Reimers, J. R. *J. Am. Chem. Soc.* **2007**, *129*, 14532–14533.
(17) Gronbeck, H.; Hakkinen, H. *J. Phys. Chem. B* **2007**, *111*, 3325–3327.
(18) Chaudhuri, A.; Lerotholi, T. J.; Jackson, D. C.; Woodruff, D. P.; Dhanak, V. *Phys. Rev. Lett.* **2009**, *102*, 126101–126104.
(19) Cossaro, A.; Mazzarello, R.; Rousseau, R.; Casalis, L.; Verdini, A.; Kohlmeyer, A.; Floreano, L.; Scandolo, S.; Morgante, A.; Klein, M. L.; Scoles, G. *Science* **2008**, *321*, 943–946.
(20) Clavilier, J.; Faure, R.; Guinet, G.; Durand, R. *J. Electroanal. Chem.* **1979**, *107*, 205–209.
(21) Maksymovych, P.; Sorescu, D. C.; Dougherty, D.; Yates, J. T., Jr. *J. Phys. Chem. B* **2005**, *109*, 22463–22468.
(22) Soler, J. M.; Artacho, E.; Gale, J. D.; Garcia, A.; Junquera, J.; Ordejon, P.; Sanchez-Portal, D. *J. Phys.: Condens. Mater.* **2002**, *14*, 2745–2779.
(23) Voznyy, O.; Dubowski, J. J. *Langmuir* **2009**, *25*, 7353–7358.
(24) Sellers, H.; Ulman, A.; Shnidman, Y.; Eilers, J. E. *J. Am. Chem. Soc.* **1993**, *115*, 9389–9401.

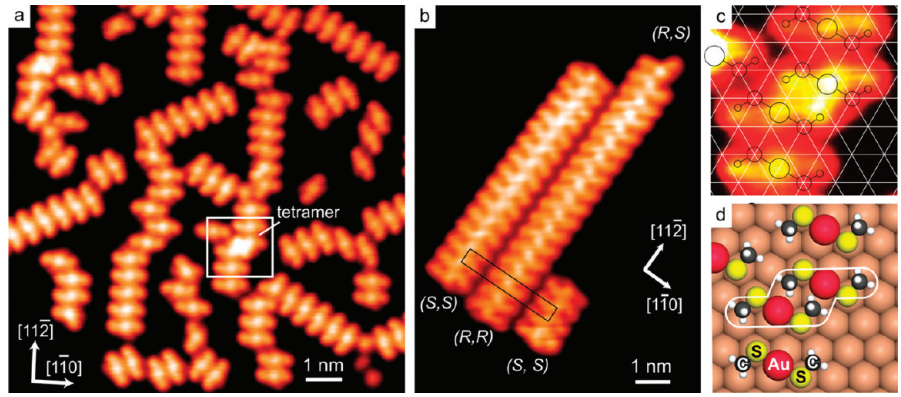

Figure 2. STM images of (a) intermediate coverage of methylthiolate on Au(111) revealing the coexistence of stripes, single *cis*- and *trans*-complexes, and tetramers ($T > 200$ K during self-assembly). (b) Striped phase of propylthiolate with $(11 \times \sqrt{3})$ unit cell, formed by thermal dissociation and subsequent self-assembly of C_3H_7SH molecules at $T > 250$ K. The tetramer unit (c) and its schematic structure (d) correspond to the outlined area in panel (a).

as detailed in Figure 1f,g. The $(CH_3S)_2Au$ complex comprises the S-atoms of either the same type, *R* or *S*, yielding a *trans*-$(CH_3S)_2Au$ isomer (Figure 1f), or of opposite type, *R* and *S*, yielding a *cis*-$(CH_3S)_2Au$ (Figure 1g). The difference in the adsorption energy between *cis*- and *trans*-complexes, calculated here by DFT, is less than 0.1 eV; that is, they are thermodynamically equivalent. However, the barrier to switch between the two configurations, calculated using the nudged elastic band method, amounts to 0.50 eV (at half of saturation coverage). Thermally activated *cis*−*trans* isomerization should therefore become facile already at $T = 200$ K, which is the temperature where the self-assembly of the thiolate species takes place in our experiments. The existence of both *cis*- and *trans*-$(CH_3S)_2Au$ complexes is confirmed by STM images obtained at low and intermediate coverages of methylthiolate (Figure 1a−c).

The adatom complexes of methylthiolate readily cluster at low coverages, forming 1D-stripes up to 15 $(CH_3S)_2Au$ in a row along the $\langle 11\bar{2}\rangle$ direction (Figure 1a and Figure 2a). The clustering is driven by the attractive interaction between *trans*-$(CH_3S)_2Au$ complexes (calculated to be ~ 0.09 eV per complex[9]) when they are located at a distance of $\sqrt{3}a$ along the $\langle 11\bar{2}\rangle$ direction ($a = 2.885$ Å is the gold surface lattice constant). Minimization of steric repulsion within the stripes requires all the complexes to have exactly the same *trans*-configuration, that is, to be either of *R*,*R*- or *S*,*S*-type. No evident 2D-ordering of the methylthiolate stripes is observed at intermediate coverages (Figure 2a), indicating weak or even repulsive interstripe interactions. However, the stripes of longer-chain alkylthiolates, such as propylthiolate (C_3H_7S), exhibit a pronounced 2D-order even at a low coverage as seen in Figure 2b. The 1D stripes assemble along the $\langle 1\bar{1}0\rangle$ direction, normal to the stripe-axis. This is likely due to an increase of the van der Waals interactions between the hydrocarbon tails compared to methylthiolate. The 2D-ordered striped phase possesses a rectangular $(n \times \sqrt{3})$ unit cell, where *n* is integer.[1,25] Although 2D-stripe phases have been routinely observed for longer alkanethiolates, an intriguing property discovered here is a chiral recognition between the 1D stripes. It is manifested in the alternating type of the stripes between *R*,*R*- and *S*,*S*- symmetries (Figure 2b) arising in order to reduce the steric repulsion between stripes.

We naturally expect that the self-assembled structures beyond striped phases will evolve from the building blocks available within the striped phase and would at some point coexist with the stripes. The self-assembly at high coverage may involve *cis*−*trans* isomerization of the $(CH_3S)_2Au$ complexes, their rearrangement on the surface, or occurrence of new sulfur-to-gold bonding motifs. We have found that increasing methylthiolate coverage past the striped phase brings out a new structural motif, formed when two stripes, whose axes are displaced by $1.5a$ distance along the $\langle 1\bar{1}0\rangle$ direction, meet end-to-end as illustrated in Figure 2a,c,d. Such a 'tetramer' comprises two slightly overlapping *trans*-$(CH_3S)_2Au$ complexes. Steric repulsion between the CH_3-group in one complex and the Au-adatom in the other makes two of the four CH_3 groups slightly buckled, increasing their apparent height in STM (Figure 2a). The STM image of the tetramer is very similar to the building block of the (3×4) phase previously reported by Kondoh et al.[26]

At near-saturation coverage, tetramers become a prevalent species while the length of the 1D-stripes decreases (Figure 3a). The tetramers form local arrangements with the periodicity of either $(3 \times 4\sqrt{3})$ (Figure 3b) or (3×4) (Figure 3c). Both unit-cells correspond to saturation coverage of CH_3S and differ only by the relative positions and chirality of the constituent tetramers. The (3×4) phase comprises tetramers of identical spatial configuration (all *R*,*R* or all *S*,*S* complexes), arranged to yield the (3×4) sublattice of the sulfur atoms (Figure 3e). In contrast, the $(3 \times 4\sqrt{3})$ phase comprises rows of the *R*,*R* and *S*,*S* tetramers alternating along the $\langle 11\bar{2}\rangle$ direction, yielding the $(\sqrt{3} \times \sqrt{3})R30°$ sublattice of the sulfur atoms (Figure 3d). Our DFT calculations show that the (3×4) periodicity is more stable than $(3 \times 4\sqrt{3})$ by $\sim$0.12 eV per adatom complex, which is consistent with their coexistence on the surface. The (3×4) phase of methylthiolate has previously been reported in several works.[26,27] However, to the best of our knowledge, this is the first observation of the $(3 \times 4\sqrt{3})$ unit cell.

The STM observations may seem inconsistent with the results of diffraction techniques where the signal is averaged over a large surface area, such as low energy electron diffraction (LEED)[5,26,27] and grazing-incidence X-ray diffraction (GIXRD).[10] These studies have reported the formation of the $(\sqrt{3} \times \sqrt{3})R30°$ phase at the saturation coverage of methylthiolate on Au(111). The use of adatom complexes to build up the SAM requires a unit cell that is bigger than that of $(\sqrt{3} \times \sqrt{3})R30°$. To resolve this discrepancy, Mazzarello et al.[10] proposed a different structural model, where the adatom-bonded

(25) Poirier, G. E. *Chem. Rev.* **1997**, *97*, 1117–1127.
(26) Kondoh, H.; Nozoye, H. *J. Phys. Chem. B* **1999**, *103*, 2585–2588.
(27) De Renzi, V.; Di Felice, R.; Marchetto, D.; Biagi, R.; del Pennino, U.; Selloni, A. *J. Phys. Chem. B* **2004**, *108*, 16–20.

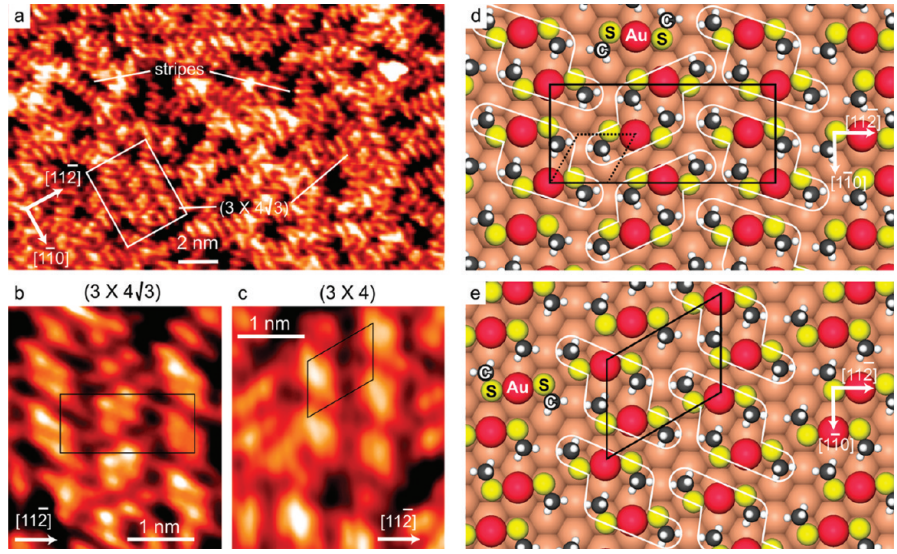

Figure 3. High-coverage self-assembled structures of methylthiolate on Au(111) obtained by heating the gold crystal predosed with CH_3SSCH_3 to $T > 250$ K for ~10 min. (a) The largely 1D-stripes of $(CH_3S)_2Au$ coexisting with several patches of the $(3 \times 4\sqrt{3})$ phase. (b) Close-up of the left $(3 \times 4\sqrt{3})$ patch in panel (a). (c) Close-up of the (3×4) patch found in the surface area adjacent to the area shown in panel (a). (d and e) DFT-optimized structural models of the proposed saturated $(3 \times 4\sqrt{3})$ and (3×4) phases, respectively, with unit cells indicated in black and $(\sqrt{3} \times \sqrt{3})R30°$ unit cell as dotted black. White outlines correspond to tetramer patterns observed experimentally in panels (b) and (c).

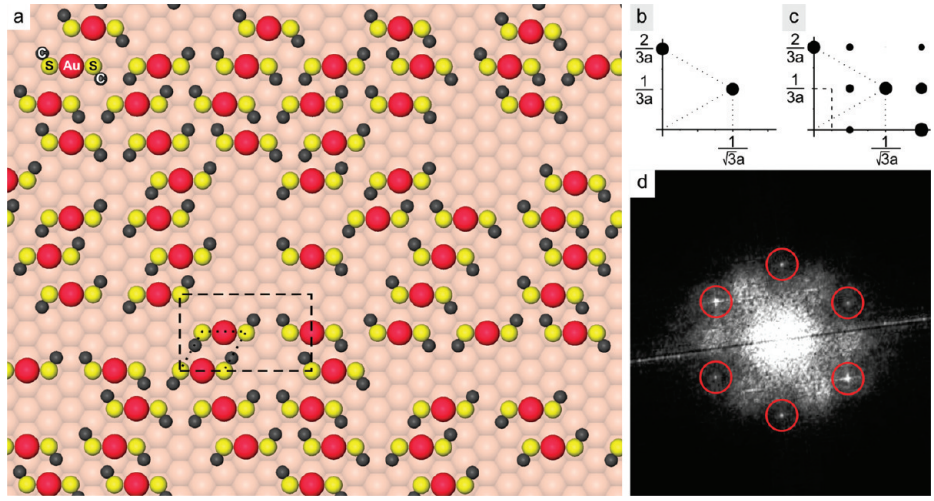

Figure 4. (a) Structural model of the disordered phase derived from $(3 \times 4\sqrt{3})$. Dashed and dotted lines show the $(3 \times 4\sqrt{3})$ and $(\sqrt{3} \times \sqrt{3})R30°$ unit cells, respectively. Calculated GIXRD patterns of this phase exhibiting the $(\sqrt{3} \times \sqrt{3})R30°$ symmetry (b) and of the ordered $(3 \times 4\sqrt{3})$ phase (c). (d) Fourier transform of the STM image in Figure 3a featuring sharp $(\sqrt{3} \times \sqrt{3})R30°$ peaks and a diffuse background due to disorder.

methylthiolate complexes coexist in a dynamic equilibrium with the bridge-bonded thiolate species adjacent to vacancy, creating a disordered monolayer. Upon averaging, the disordered structure satisfies the $(\sqrt{3} \times \sqrt{3})R30°$ symmetry observed by GIXRD. Our STM images obtained at low and intermediate coverages of methylthiolate (Figures 1a and 2a) show that the dominant species on the surface are *trans*- and *cis*-$(CH_3S)_2Au$ complexes. This fact alone does not rule out the possible existence of the vacancies or other kinds of CH_3S species at the saturation coverage. However, we have found that the concept of disorder can be used to generate a macroscopically observed $(\sqrt{3} \times \sqrt{3})R30°$ symmetry using only methylthiolate−adatom complexes. In particular, we assumed the existence of the $(3 \times 4\sqrt{3})$ phase with a reduced long-range order at the expense of smaller coverage (~75% of saturation coverage), as shown in Figure 4a. Simulated in-plane GIXRD pattern of this structure (Figure 4b, for details see Supporting Information) exhibits only $(\sqrt{3} \times \sqrt{3})R30°$ peaks despite the apparent lack of this unit-cell on the local scale within the structure. Since GIXRD is dominated by diffraction from Au adatoms;[3,23] the latter must occupy the $\sqrt{3}$ sublattice within the self-assembled layer. This requires all the $(CH_3)_2Au$ complexes to be aligned along the same direction, since otherwise the adatoms end up on the sites belonging to a $(\sqrt{3}/2 \times \sqrt{3}/2)R30°$ lattice (see Supporting Iinformation), generating a corresponding pattern in GIXRD. For comparison, the ordered $(3 \times 4\sqrt{3})$ phase produces the $(3 \times 2\sqrt{3})$ GIXRD pattern (Figure 4c) corresponding to the symmetry of adatoms, while being largely insensitive to the positions of S and C atoms. This pattern is practically identical to that of the $c(4 \times 2)$ phase of longer thiols.[8,19] The notion of the disordered structure that produces a well-ordered pattern in reciprocal space is also consistent with our STM images at near-saturation coverage; for example, in Figure 3a, the Fourier transform of which also shows sharp $(\sqrt{3} \times \sqrt{3})R30°$ spots (Figure 4d).

Is it also possible to use the adatom complex to construct the SAMs of longer-chain alkanethiolates? The (3×4) phase was also reported in an STM study of ethanethiolate monolayers,[28] although with a significantly different STM contrast than for methylthiolate. Our simulations of the ethylthiolate (3×4) structure with the same arrangement of adatom complexes as for methylthiolates are in excellent agreement with the reported experimental images (Supplementary Figure S2). However, both (3×4) and $(3 \times 4\sqrt{3})$ phases observed for methylthiolate will be highly unstable when more than two carbon atoms build up the hydrocarbon tail, since the *trans*-configuration of the adatom complex would introduce significant steric hindrance with longer hydrocarbon tails. This steric hindrance can, however, be largely overcome if all *trans*-complexes within the $(3 \times 4\sqrt{3})$ phase are transformed into their *cis*-isomers. The resulting arrangement of the S−Au−S bonds bears the $c(4 \times 2)$ periodicity, which makes this structure a possible candidate for the corresponding phase of long-chain alkanethiolates on Au(111). Our previous work addressing the steric commensurability of various possible dense phases of longer thiols with the $(3 \times 2\sqrt{3})$ unit cell of gold surface suggested the *cis*-conformers of thiolate−adatom−thiolate complexes as one of the few viable packings and the only one thermodynamically stable, considering significant energy cost of adatoms formation.[23] The *cis*-based $c(4 \times 2)$ structure was also proposed by Grönbeck et.al.[15] for methylthiolate SAMs and by Torres et al.[29] for ethylthiolate SAMs, based on the total energy calculations. However, as we have shown here, the preferred arrangements of methylthiolate are based on *trans*- rather than *cis*-adatom complexes.

To build up the high-coverage self-assembled structures of alkanethiolate of the RS-Au-SR adatom complexes, the gold surface has to supply 1/6 ML of gold adatoms. Previously, we showed that the $(22 \times \sqrt{3})$ herringbone reconstruction provides the adatoms required for thiolate self-assembly at low coverage.[9] However, the reconstruction can only provide for 0.04 ML of adatoms, while the rest of them must be released from single atom steps and surface terraces. This is consistent with the observation of surface pits and eroded surface terraces accompanying thiolate self-assembly.[4,7] The surface area of the etch pits estimated from images in previous works is 0.04−0.1 ML,[23] which supports this hypothesis. The total density of gold adatoms released from the surface will, in general, be difficult to determine since quantitative analysis of step erosion is not straightforward and it will also depend on initial step density on the Au(111) surface.

(28) Kawasaki, M.; Nagayama, H. *Chem. Lett.* **2001**, *30*, 942–943.
(29) Torres, E.; Blumenau, A. T.; Biedermann, P. U. *Phys. Rev. B* **2009**, *79*, 075440–075445.

4. Conclusions

We have developed structural models for the self-assembled phases of methylthiolate on the Au(111) surface at *all* coverages in terms of the same basic building block of two CH_3S fragments linked by a gold adatom. The stereochemical properties of the $(CH_3S)_2Au$ complexes are found to play a critical role in the interaction between the complexes and the resulting formation of the self-assembled patterns. We have found that the adatom complexes can form local arrangements with the $(3 \times 4\sqrt{3})$ or (3×4) unit-cells, both providing the saturation coverage of CH_3S-species on the Au(111) surface. Introducing the long-range disorder into the $(3 \times 4\sqrt{3})$ phase, which is consistent with our STM images at near-saturation coverages, allows one to obtain a macroscopically averaged GIXRD pattern of $(\sqrt{3} \times \sqrt{3})R30°$. Upon *trans*−*cis* isomerization of the constituent $(C_nH_{2n+1}S)_2Au$ complexes, the $(3 \times 4\sqrt{3})$ phase attains the $(3 \times 2\sqrt{3})$ symmetry and may therefore naturally explain the $c(4 \times 2)$ structure of the longer alkanethiolates. We anticipate that the results presented here will help to gain a complete picture of the alkylthiolate self-assembly process, particularly, the reaction mechanisms behind the incorporation of the gold adatoms into alkylthiolate complexes, the chiral recognition within the striped phase, discovered here, and the formation of densely packed monolayers. We further envision the applicability of the key concepts behind alkanethiol self-assembly in other molecular systems and a potential to engineer novel self-assembled functionality, such as strong surface magnetism or new electronic properties, using substitutional metal adatoms.

Acknowledgment. The funding for this research has been provided by the Natural Sciences and Engineering Research Council of Canada - STPGP 350501-07 and Canada Research Chair in Quantum Semiconductors Program (J.J.D.). P.M. and J.T.Y: Supported by the W. M. Keck Foundation and by the Army Research Office. P.M.: Research performed in part, as a Eugene P. Wigner Fellow and staff member at the Oak Ridge National Laboratory. Computational resources were provided by the Réseau québécois de calcul de haute performance (RQCHP).

Supporting Information Available: GIXRD simulation details, structure and simulated STM image of ethylthiolate SAMs. This material is available free of charge via the Internet at http://pubs.acs.org.

JA902629Y